MODELING OF A MICROFLUIDIC ANALOG OF THE FOUR-ROLL MILL FOR MATERIALS CHARACTERIZATION

F. R. Phelan Jr. and S. D. Hudson
Polymers Division
National Institute of Standards and Technology
Gaithersburg, MD 20899

Abstract[1]

The fluid dynamics of channel geometries for liquid state materials characterization in microfluidic devices are investigated. A pressure driven microchannel device is sought that has an adjustable flow type, approximating the function of the four-roll mill. In particular, classes of channel flows in which the full range of linear flows (extension, shear and rotation) can be approximated in the neighborhood surrounding a stagnation point are investigated using finite element flow simulation and flow classification criteria. A class of flow geometries is identified which makes use of opposing, laterally offset fluid streams that produce a stagnation point in the center of the geometry.

Introduction

Fluid flow in microfluidic devices is becoming more and more common, driven by the miniaturization of many technologies [1-3]. Such devices afford a number of advantages over conventional methods, including greater speed, replacement of multiple manual steps, conservation of expensive and/or limited quantity reagents, and reduced human error.

The goal in this study is to apply existing microfluidics technology to the development of a microfluidic device for liquid state materials characterization. A variety of applications for such a platform can be anticipated ranging from such traditional areas as interfacial dynamics, viscosity measurement, molecular stretching, and crystallization, to newer areas such as dispersion/aggregation of nanoparticle fillers, and flow induced changes in biological cells.

The ideal types of flow for the characterization of fluids are linear flows which are described by the stream function and corresponding velocity vector

$$\psi = \frac{1}{2}\left(\xi\gamma x^2 - \gamma y^2\right) \qquad (1.1)$$

$$\underline{v} = \left(\gamma y, \xi\gamma x\right) \qquad (1.2)$$

The nature of these kinematics are characterized by the constants ξ and γ[4]. The quantity ξ is the flow type, and indicates the nature of the deformation experienced by the fluid; the flow is extensional for $\xi = 1$, shear for $\xi = 0$, and pure rigid body rotation for $\xi = -1$. The quantity γ is the flow strength, and indicates the magnitude of the velocity gradient relative to the flow type.

A number of devices that approximate particular modes of linear flows at the macroscale are available [5-14]. The device that comes closest to the desired functionality is the four roll mill. While this is primarily thought of as a device for producing planar extension ($\xi = 1.0$), it can also be used to provide mixed flows for $0.2 < \xi < 1.0$ [7-8], and rotational flows where $\xi \sim -1$ [9]. However, the four roll geometry is inadequate for producing simple shear ($\xi = 0$), and difficulties can be anticipated in trying to produce and control a miniature device with moving parts. This leads us to seek a design based on channel flow.

In this study, a pressure driven microchannel device is sought that has an adjustable flow type, approximating the function of the four-roll mill, but with the ability to produce a broader range of kinematics. In particular, we investigate classes of channel flows in which the full range of linear flows can be approximated in the neighborhood surrounding a stagnation point. To evaluate various candidate geometries, finite element flow simulations in the low Reynolds number limit were undertaken. Flow classification criteria [4] were then used to delineate combinations of geometry and boundary conditions for which the flow type can be adjusted between shear and extension in the neighborhood surrounding the stagnation point, while providing adequate flow strength.

A class of flow geometries is identified which makes use of opposing, laterally offset fluid streams, that produce a stagnation point. Opposing fluid streams are necessary to produce a stagnation point. While this is normally a means to generate pure extension, the lateral offset which is also employed introduces vorticity at the stagnation point, enabling the generation of shear and even rotation. The flow type can be manipulated by varying the pressure boundary conditions at the inlets and outlets of the flow.

Modeling

Flow Simulation

To evaluate various candidate geometries, flow was simulated using the finite element method at the zero Reynolds number limit. All flows were assumed to be steady and two-dimensional. Modeling was carried out using the commercial finite element packages[2] FIDAP [15] and FlexPDE [16]. The governing equations solved by FIDAP are the Navier-Stokes equations with the incompressible condition

$$-\nabla p+\eta\nabla^2\underline{u}=0 \tag{1.3}$$

$$\nabla\cdot\underline{u}=0 \tag{1.4}$$

FlexPDE makes use of the alternative incompressible formulation

$$\nabla^2 p=-\nabla\cdot\nabla\cdot\left(\rho\underline{u}\underline{u}\right)+\beta(\nabla\cdot\underline{u}) \tag{1.5}$$

where β is a large value chosen such that $\nabla\cdot\underline{u}$ is sufficiently small.

Flow Classification in Non-Homogeneous Flows

In a linear flow, the velocity gradient tensor is constant and the flow type is uniform, which makes measurement of flow properties as a function of deformation rate unambiguous. In practice, linear flows are not perfectly achievable, and we seek to approximate linear flows in the neighborhood of a stagnation point to achieve the desired flow kinematics. Therefore, generalized flow classification criteria for discerning the flow type as a function of position in non-homogeneous flows are a useful tool for determining the utility of various complex flow fields for producing a correct flow type in a region surrounding a stagnation point.

A suitable objective criterion for classifying the flow type in complex flows has been developed by Astarita [4]. The type of a flow may be determined by computing the non-dimensional number

$$\Xi=\frac{\underline{\underline{D}}:\underline{\underline{D}}+\underline{\underline{W}}:\underline{\underline{W}}}{\underline{\underline{D}}:\underline{\underline{D}}-\underline{\underline{W}}:\underline{\underline{W}}} \tag{1.6}$$

where $\underline{\underline{D}}$ is the stretching tensor given by

$$\underline{\underline{D}}=\frac{1}{2}\left(\nabla\underline{v}+\nabla\underline{v}^T\right) \tag{1.7}$$

and $\underline{\underline{W}}$ is the a tensor defined as

$$\underline{\underline{W}}=\underline{\underline{\omega}}-\underline{\underline{\Omega}} \tag{1.8}$$

where

$$\underline{\underline{\omega}}=\frac{1}{2}\left(\nabla\underline{v}-\nabla\underline{v}^T\right) \tag{1.9}$$

$$\underline{\underline{\Omega}}=\frac{d\underline{\underline{E}}}{dt}\cdot\underline{\underline{E}}^{-1} \tag{1.10}$$

In the definition of $\underline{\underline{W}}$, $\underline{\underline{\omega}}$ is the vorticity tensor, $\underline{\underline{E}}$ is the matrix of right eigenvectors of $\underline{\underline{D}}$, and the tensor $\underline{\underline{\Omega}}$ describes the rate of rotation of the principal axes of $\underline{\underline{D}}$.

Like the constant ξ in linear flows, the variable Ξ has a value equal to 1 in purely extensional flows, 0 in shear flows, and -1 in a pure rigid body rotation. Values between 1 and 0 indicate a mixture of extension and shear, and values between 0 and –1 indicate mixed shear and rotation. For steady two-dimensional flows, the stretching and vorticity tensors can be generalized as

$$\underline{\underline{D}}=\begin{bmatrix}\varepsilon & \gamma\\ \gamma & -\varepsilon\end{bmatrix} \tag{1.11}$$

$$\underline{\underline{\omega}}=\begin{bmatrix}0 & \omega\\ -\omega & 0\end{bmatrix} \tag{1.12}$$

and $\underline{\underline{\Omega}}$ and $\underline{\underline{W}}$ take on the anti-symmetric forms

$$\underline{\underline{\Omega}}=\begin{bmatrix}0 & \Omega\\ -\Omega & 0\end{bmatrix} \tag{1.13}$$

$$\underline{\underline{W}}=\begin{bmatrix}0 & W\\ -W & 0\end{bmatrix} \tag{1.14}$$

where $W=\omega-\Omega$ and

$$\Omega=\frac{\gamma\left(u\frac{\partial\varepsilon}{\partial x}+v\frac{\partial\varepsilon}{\partial y}\right)-\varepsilon\left(u\frac{\partial\gamma}{\partial x}+v\frac{\partial\gamma}{\partial y}\right)}{2\sqrt{\varepsilon^2+\gamma^2}} \tag{1.15}$$

In this case, Ξ is given by the expression

$$\Xi=\frac{\varepsilon^2+\gamma^2-W^2}{\varepsilon^2+\gamma^2+W^2} \tag{1.16}$$

If the linear flow kinematics given by Eq. (1.2) are used in Eq. (1.6), one finds that Ξ and the linear flow type ξ are simply related by the expression $\xi=\frac{\Xi}{1+\sqrt{1-\Xi^2}}$ over the bounds $-1\le\Xi\le1$.

For classifying flow strength, there are a number of possible criteria. An objective measure, useful for comparing the relative strength of different flow fields is the maximum eigenvalue of the stretching tensor given by

$$\lambda=\sqrt{\varepsilon^2+\gamma^2} \tag{1.17}$$

which is equivalent to $\sqrt{\frac{1}{2}tr\underline{\underline{D}}^2}$. Based on this, a relative flow strength can be defined as

[2] Identification of a commercial product is made only to facilitate reproducibility and to adequately describe procedure. In no case does it imply endorsement by NIST or imply that it is necessarily the best product for the procedure.

$$S_r = \frac{\lambda}{\lambda_{ref}} \qquad (1.18)$$

where λ_{ref} is the flow strength at some reference point in the flow field. In what follows, we classify different flow fields using Eq. (1.18), taking the reference flow strength to be an average flow strength at the inlet or outlet of a channel geometry. This enables comparison of the strength of deformation in the stagnation region with the deformation in the pressure driven channels that drive the flow.

Flow Geometry and Simulation Results

In determining the parameters of a flow device that could be used to generate a range of approximately linear flows in the region surrounding a stagnation point, it was recognized that creating a flow with a stagnation point requires the use of oppositely directed fluid streams, which is generally a means to produce extensional flow. However, as mentioned above, by creating lateral offset between the opposing streams, shear and even rotation can be produced as well. We make use of this principle in our investigation.

Parallel, Laterally Offset Jets with Transverse Flow

The geometry together with boundary conditions studied here are depicted in Figure 1. Overall the geometry represents a modification of the basic cross flow device. Two important modifications are evident. First, the flow channels in the vertical direction are asymmetrically offset from the center of the channel on the top and bottom of the geometry by distances of $\pm H_2/2$, respectively. Second, the horizontal channels are split by a spacer plate of thickness h_{fin}. This provides two extra flow channels in the horizontal direction. The upper and lower spacer plates are offset by a distance d_{off}.

The flow geometry has three different boundary pressures, P_{in}, P_1, and P_2. The pressure P_{in} represents a pressure that remained fixed during a simulation, while the values of P_1 and P_2 represent pressures that were allowed to vary. The flow type at the stagnation point in this geometry is solely a function of the ratio $P_{rat} = \frac{\Delta P_1}{\Delta P_2}$, where $\Delta P_1 = P_{in} - P_1$, $\Delta P_2 = P_{in} - P_2$. By specifying values for P_{in}, P_{rat} and $P_{mag} = \Delta P_2$, values for P_1, and P_2 were set as $P_1 = P_{in} - P_{mag} \cdot P_{rat}$ and $P_2 = P_{in} - P_{mag}$. The relevant geometric and boundary condition parameters used in the simulations to be presented are listed in Table 1.

Plots of flow type and relative flow strength at the stagnation point as a function of P_{rat} are shown in Figures 2-3. Figure 2 shows that the entire range of flow types can be reached. For highly negative pressure ratios the flow type has a value that is negative, indicating a high degree of rotation. As P_{rat} decreases towards zero, the amount of rotation is continually reduced and the extensional flow type value of unity (extension) is reached at a pressure ratio of approximately -1. As the pressure ratio further increases and becomes positive, a shear flow type of zero at the stagnation point is eventually realized for a pressure ratio value of approximately 2. The relative flow strength depicted in Figure 3 is taken relative to the average flow strength at the inlet of the flow. The plot shows the flow strength continually rises (almost linearly) with increase in the pressure ratio. Thus, the flow strength value is highest for the case of shear (0.6). The value for extension is approximately 0.23. Values are tabulated in Table 2.

Discussion

In developing a microfluidic device for liquid state materials characterization, the most basic need is to have a suitable flow geometry for deforming the fluid in a controlled manner. Ideally, such a geometry would be able to supply a full range of linear flows in which the velocity gradient tensor is constant and the flow type is uniform. Since in practice, linear flows are not perfectly achievable, we have sought to investigate classes of channel flows in which the full range of linear flows can be approximated in the neighborhood surrounding a stagnation point. The long fluid residence time surrounding a stagnation flow region provides a stable environment for material observation and measurement, and allows us to ignore the inhomogeneities present in complex flows, provided that the stagnation region flow gradients can be made suitably uniform.

Using a combination of finite element simulation and flow classification theory, a class of flow geometries that fit the above criteria has been determined. It is able to produce the full range of linear flow kinematics at the stagnation point, with varying, but in all cases acceptable degree of flow strength. In the results presented, complete optimization of the flow geometry parameters has not been attempted as our primary goal in this initial study was simply to identify geometry and boundary condition combinations that allow us to achieve the basic goal of generating a full range of flow types. This, in coordination with experimental testing, is part of our ongoing work.

There are a number of other items that will need to be examined in future work. First, our initial results presented here have considered the system to be 2-D in nature, as is done for example with the four roll mill. However, shear in the third direction is likely to have some effect and will be taken into account by means of 3-D flow simulation. In addition, non-Newtonian flow behavior will have to be addressed when working with polymer systems.

Summary and Conclusions

In this study, the fluid dynamics of pressure driven flow in microchannels was studied for the purpose enabling the design of a microfluidic, liquid state, materials characterization device. Channel flows in which a full range of linear flows could be approximated in the neighborhood surrounding a stagnation point were investigated be means of finite element flow simulations, together with flow classification criteria. A class of flow geometries was identified which makes use of opposing, laterally offset fluid streams. The opposing fluid streams are necessary to produce a stagnation point, and the lateral offset is necessary in order to introduce rotation into the flow to produce shear. Geometry optimization in coordination with experimental testing is underway.

References

1. Thorsen, T., S.J. Maerkl, and S.R. Quake, "Microfluidic Large-Scale Integration", Science, 298, p.580, (2002).
2. Ouellette, J., "A New Wave of Microfluidic Devices", The Industrial Physicist, p. 14, (August/September 2003).
3. Chow, A.W., "Lab-on-a-Chip: Opportunities for Chemical Engineering", AICHE Journal, 48(8), p. 1590, (2002).
4. Astarita, G., "Objective and generally applicable criteria for flow classification", Journal of Non-Newtonian Fluid Mechanics, 6, p. 69-76, (1979).
5. Taylor, G.I., "The formation of emulsions in definable fields of flow", Proc. Roy. Soc. London Ser. A, 146, p. 501, (1934).
6. Fuller, G.G. and L.G. Leal, "Flow birefringence of concentrated polymer solutions", J. Poly. Sci., Poly. Phys., 13, p. 43, (1981).
7. Bentley, B.J., and L.G. Leal, "A computer controlled four-roll mill for investigations of particle and rope dynamics in tow-dimensional linear shear flows", J. Fluid Mech., 167, p. 219, (1986).
8. Bentley, B.J., and L.G. Leal, "An experimental investigation of drop deformation and breakup in steady, two-dimensional flows", J. Fluid Mech., 167, p. 241, (1986).
9. Higdon, J.L.L., "The Kinematics of the Four Roll Mill," Phys. Fluids A, 5(1), p. 274, (1993).
10. Frank, F.C. and M.R. Mackley, "Localized flow birefringence of polyethylene oxide solutions in a two roll mill", Journal of Polymer Science A2, 14,1121-1131 (1976).
11. Hills, C.P., "Flow Patterns in a Two-Roll Mill", The Quarterly Journal of Mechanics and Applied Mathematics, 55(2), p. 273, (May 2002).
12. Berry, M.V. and M.R. Mackley, "The six roll mill: Unfolding an unstable persistently extensional flow," Phil. Trans. Royal Soc. (Lond.), 287, 1337, 1-16 (1977).
13. Keller, A. and J.A. Odell, Colloid Poly. Sci., 263, p. 181, (1985).
14. Bird, B., R.A. Armstrong, and O. Hassager, Dynamics of Polymeric Liquids, Volume 1, Wiley, (1982).
15. Fidap User's Manual, Fluent, Inc., Evanston, IL, (2003).
16. FlexPDE User's Manual, PDE Solutions, Inc. (2003).

Inlet Width (H_{in})	**Inlet/Outlet Width 1 (H_1)**	**Inlet/Outlet Width 2 (H_2)**	**Fin Width (H_{fin})**	**Channel Length (L)**	**Offset Distance**	**Pressure Magnitude (P_{mag})**	**Inlet Pressure (P_{in})**
2	1	2	0.05	5	0.5	1.0	0

Table 1. Geometry parameters and boundary conditions used for the parallel, laterally offset, channel geometry, with transverse flow channels.

Case	**Pressure Ratio (P_{rat})**	**Pressure 1 (P_1)**	**Pressure 2 (P_2)**	**Flow Type**	**Relative Flow Strength**
Extension	-0.9	0.9	-1	0.9995	0.233
Shear	-2.2	2.2	-1	-0.0044	0.596

Table 2. Values for flow type and flow strength at the stagnation point for the parallel, laterally offset, channel geometry, with transverse flow channels, at offset distances mostly closely corresponding to the cases of extension and shear.

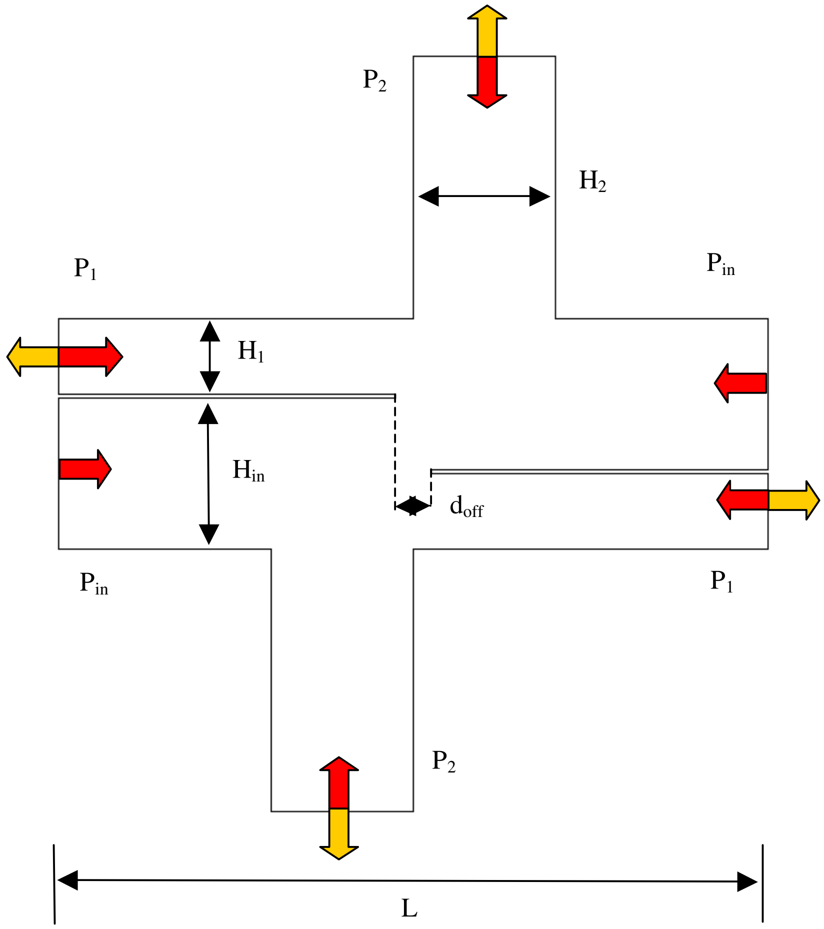

Figure 1. Geometry, parameters and boundary condition for the parallel, laterally offset, jet geometry, with transverse flow channels. Parameters used in the simulation are listed in Table 1.

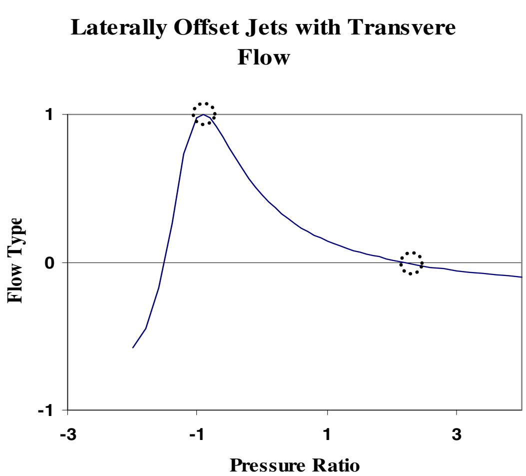

Figure 2. Flow type as a function of the pressure ratio for the parallel, laterally offset, channel geometry, with transverse flow channels.

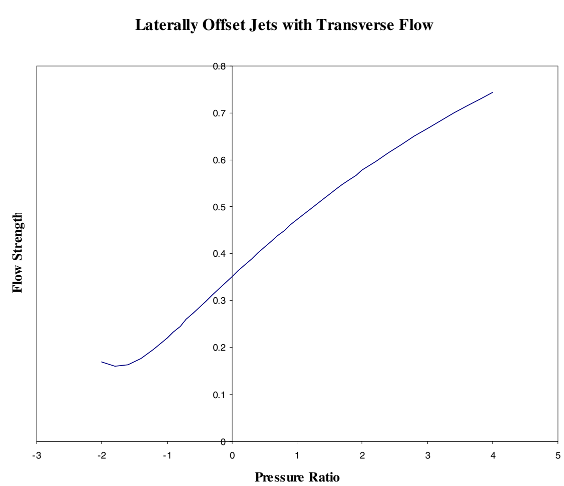

Figure 3. Relative flow strength as a function of the pressure ratio for the parallel, laterally offset, channel geometry, with transverse flow channels.